FEBS 25816 FEBS Letters 514 (2002) 37–43

The minimal tRNA: unique structure of *Ascaris suum* mitochondrial $tRNA^{Ser}_{UCU}$ having a short T arm and lacking the entire D arm

Takashi Ohtsuki, Gota Kawai[a,1], Kimitsuna Watanabe[a,*]

[a] *Department of Chemistry and Biotechnology, Graduate School of Engineering, The University of Tokyo, 7-3-1 Hongo, Bunkyo-ku, Tokyo 113-8656, Japan*

Received 25 November 2001; accepted 27 November 2001

First published online 1 February 2002

Edited by Lev Kisselev

Abstract The tertiary structure of *Ascaris suum* mitochondrial $tRNA^{Ser}_{UCU}$ was examined by nuclear magnetic resonance analysis using its transcript, since $tRNA^{Ser}_{UCU}$, lacking the D arm and possessing a truncated T arm, is the shortest of all the known tRNAs. Most basepairs in the proposed secondary structure of $tRNA^{Ser}_{UCU}$ were shown to exist, but the connector region comprising the truncated D loop and the extra loop was flexible. This flexibility, would enable adjustment of the mutual distance between the 3′-terminus and the anticodon consistent with that of usual tRNAs. Thus, $tRNA^{Ser}$UCU appears to function in a similar way to that of usual tRNAs in the ribosome.

Key words: Unusual tRNA; Mitochondrion; Nematode; Nuclear magnetic resonance; Stable isotope; *Ascaris suum*

1. Introduction

All nematode mitochondrial (mt) tRNAs except for $tRNAs^{Ser}$ are known to possess extremely unusual secondary structures lacking the entire T arm [1–6]. $tRNAs^{Ser}$, comprising $tRNA^{Ser}_{UCU}$ and $tRNA^{Ser}_{UGA}$ (see Fig. 1c) [1–3,6], however, possess the T arm but lack the D arm, as do all other metazoan mt $tRNAs^{Ser}_{GCU}$ [7–9]. Furthermore, the T arm of nematode mt $tRNAs^{Ser}$ is extremely short (consisting of 10–13 residues). Thus, these tRNAs look to be the most simplified structures. In particular, *Ascaris suum* mt $tRNA^{Ser}_{UCU}$, whose chain length is 54 mer, is one of the shortest of all the tRNAs so far elucidated [9]. It has been reported from mt genome research that brachiopod mt $tRNA^{Ser}_{UGA}$ (lacking the D arm [10]) and spider mt $tRNA^{Val}$ (lacking the T arm [11]) also consist of 54 residues; however, these tRNAs have not been detected at the RNA level. The nucleotide sequence including modified nucleotides of *A. suum* mt $tRNA^{Ser}_{UCU}$ (Fig. 1a) has already been determined, and its higher order structure analyzed using enzymatic probing [4]. A structural study using computer modeling on metazoan mt $tRNAs^{Ser}$ lacking the D arm suggested that the acceptor–anticodon interstem angle is larger than the rectangle which the normal L-shaped tRNA takes, if it is assumed that the mutual distance between the 3′-terminus and the anticodon was preserved [12]. In that computer modeling, the interstem angle of nematode *Caenorhabditis elegans* mt $tRNA^{Ser}_{UGA}$ was extremely large [12].

The higher order structures and biological properties of such tRNAs with extremely short chain lengths have not been adequately clarified. In this work, *A. suum* mt $tRNA^{Ser}_{UCU}$ was analyzed by nuclear magnetic resonance (NMR) spectroscopy to obtain more detailed information about its tertiary structure. At first, NMR spectra of *A. suum* mt $tRNA^{Ser}_{UCU}$ synthesized by T7 RNA polymerase were analyzed to assign iminoproton signals. Then, unassigned residues were labeled site-specifically with a stable isotope so as to enable the assignment of the unknown iminoproton signals and also to investigate the tertiary interactions. Together with the biochemical data obtained in this study, including the binding of the tRNA to bacterial elongation factor Tu (EF-Tu), the structural features of *A. suum* mt $tRNA^{Ser}_{UCU}$ can be determined.

2. Materials and methods

2.1. Purification of native *A. suum* mt $tRNA^{Ser}_{UCU}$

A. suum total tRNAs were prepared from the body wall muscle of *A. suum* as described [4]. *A. suum* mt $tRNA^{Ser}_{UCU}$ was isolated from total tRNAs by the selective hybridization method [13] using a solid-phase DNA probe (obtained from Sci-Media, Japan) possessing a sequence complementary to the residue numbers G1 to U30 of the tRNA, and purified further by 10% denaturing polyacrylamide gel electrophoresis. A 0.98 A_{260} unit of $tRNA^{Ser}_{UCU}$ was obtained from 736 A_{260} units of *A. suum* total tRNAs. The nucleotide sequence of the tRNA was confirmed by Donis–Keller's method [14].

2.2. Preparation of *A. suum* mt $tRNA^{Ser}_{UCU}$ transcripts

The template plasmid for T7 transcription, in which the T7 RNA polymerase promoter sequence directly connected to the downstream of the $tRNA^{Ser}_{UCU}$ sequence and terminated at a *Bst*NI site was cloned into pUC19, was kindly provided by Dr. Y. Watanabe (University of Tokyo). The transcription reaction was performed at 37°C for 4 h in a reaction mixture including 40 mM Tris–HCl (pH 8.0), 6 mM $MgCl_2$, 5 mM dithiothreitol (DTT), 1 mM spermine, 0.01% Triton X-100, 50 μg/ml bovine serum albumin (BSA), 20 mM GMP, 1.2 mM ATP, 1 mM GTP, 1 mM CTP, 2 mM UTP, 3 U/ml pyrophosphatase, 2.4 μg/ml T7 polymerase and 65 μg/ml template plasmid linearized with *Bst*NI (New England Biolabs) digestion. The products were purified

*Corresponding author. Present address: Department of Integrated Biosciences, Graduate School of Frontier Sciences, The University of Tokyo, 5-1-5 Kashiwanoha, Kashiwa, Chiba 277-8562, Japan. Fax: (81)-471-36 3601.
E-mail address: kw@kwl.t.u-tokyo.ac.jp (K. Watanabe).

[1] Present address: Department of Industrial Chemistry, Chiba Institute of Technology, Chiba, Japan.

Abbreviations: BAP, *Escherichia coli* alkaline phosphatase; EF-Tu, elongation factor Tu; HMQC, heteronuclear multiple quantum correlation; mt, mitochondrial; PEG, polyethylene glycol; DTT, dithiothreitol

0014-5793/02/$22.00
PII: S0014-5793(02)02328-1

Table 1
Synthetic RNA fragments for preparation of site-specific labeled tRNAs

Labeled site	5′- or 3′-fragment[a]	RNA fragment (from 5′ to 3′)
G8	5′	GACAAAU
	3′	UUUUCAGGUCUUCUAAAUCUGUUUUGGAGAAAUCCGUUUGUUUCCAA
U11	5′	GACAAAUGUU
	3′	UCAGGUCUUCUAAAUCUGUUUUGGAGAAAUCCGUUUGUUUCCAA
U30	5′	GACAAAUGUUUUCAGGUCUUCUAAAUCUG
	3′	UUUGGAGAAAUCCGUUUGUUUCCAA
U33	5′	GACAAAUGUUUUCAGGUCUUCUAAAUCUGUUU
	3′	GGAGAAAUCCGUUUGUUUCCAA
G34	5′	GACAAAUGUUUUCAGGUCUUCUAAAUCUGUUUU
	3′	GAGAAAUCCGUUUGUUUCCAA
G35	5′	GACAAAUGUUUUCAGGUCUUCUAAAUCUGUUUUG
	3′	AGAAAUCCGUUUGUUUCCAA
G37	5′	GACAAAUGUUUUCAGGUCUUCUAAAUCUGUUUUGGA
	3′	AAAUCCGUUUGUUUCCAA

[a]3′-Fragments have an additional nucleotide at the 3′-end, because the 3′-end nucleoside should be removed before ligation reaction.

by 10% denaturing polyacrylamide gel electrophoresis. [^{15}N]GMP (Nippon Sanso, Japan) was used for G1 specific labeling.

2.3. Preparation of site-specific labeled tRNAs by chemical synthesis and enzymatic ligation

Site-specific labeled tRNAs at residues G8, U11, U30, U33, G34, G35 and G37 were prepared by enzymatic ligation of chemically synthesized RNA fragments (Table 1) and ^{15}N,^{13}C-labeled nucleotides according to the scheme in Fig. 2. Stable isotopically labeled nucleotides ([^{15}N,^{13}C]5′,3′-UDP and [^{15}N,^{13}C]5′,3′-GDP) were prepared as reported previously [5]. RNA fragments were synthesized using an Applied Biosystems 381A DNA synthesizer. Deprotection and purification of the synthetic RNAs were performed as described [15]. The general scheme of site-specific labeling using chemical synthesis and enzymatic ligation is shown in Fig. 2. To enable the fragments to serve as substrates for the RNA ligase reaction, as well as to prevent self-ligation, both ends of the 5′-fragments were dephosphorylated using *Escherichia coli* alkaline phosphatase (BAP, in Fig. 2) [5], and both ends of the 3′-fragments were phosphorylated using T4 polynucleotide kinase followed by deprivation of the 3′-end residue with $NaIO_4$ treatment [13]. The reaction mixture including 50 mM Tris–HCl (pH 7.5), 15 mM $MgCl_2$, 3.5 mM DTT, 15 μg/ml BSA, 300 μM ATP, 3–10% polyethylene glycol #6000 (PEG), 600–1200 U/ml T4 RNA ligase and 50–120 μM RNA fragments was incubated at 11°C for 14–16 h. The concentration of PEG, ligase and substrates was optimized [5] by preliminary small-scale experiments using 40–50 μl of the reaction mixture before the large scale ligations. The ligation reaction yields are summarized in Table 2. Ligated RNAs were purified by either monoQ HR 5/5 column (Pharmacia Biotech) chromatography or 10% denaturing (7 M urea) polyacrylamide gel electrophoresis.

2.4. Measurement of melting curve

The melting curves of tRNAs were measured at a wavelength of 260 nm in a buffer containing 50 mM sodium cacodylate (pH 7.0), 10 mM $MgCl_2$ and 200 mM NaCl, using a Gilford Response II spectrophotometer. *A. suum* mt tRNA^{Met} [13] was prepared as described, and *E. coli* tRNA^{Phe} was kindly provided by Dr. C. Takemoto (RIKEN, Japan).

2.5. Biochemical characterization of $tRNA^{Ser}_{UCU}$

Aminoacylation of tRNAs was carried out as described [4] using *A. suum* mt extract as the enzyme, and L-[3-^{3}H]serine (1.04 TBq/mmol) (Amersham). For the deacylation-protection assay, the charged tRNA was extracted by phenol saturated with 50 mM NaOAc (pH 4.5), twice precipitated by ethanol and dissolved with 20 mM KOAc (pH 4.5) before use. The deacylation-protection assay using the *Thermus thermophilus* EF-Tu was carried out as described [16]. Recombinant *T. thermophilus* EF-Tu was prepared as described [17].

2.6. NMR spectroscopy

Each of the tRNA samples was dissolved in 200 μl of a buffer consisting of 10 mM sodium cacodylate (pH 6.5), 0.1 mM EDTA, 150 mM NaCl, 0–15 mM $MgCl_2$ and 5% ^2H_2O. The 500 MHz ^{1}H-NMR spectra were recorded on a Bruker AMX-500 spectrometer. The water signal was suppressed by a Jump-and-Return sequence [18]. Nuclear Overhauser enhancement spectroscopy (NOESY) spectra were recorded at a mixing time of 120 ms by using a standard pulse sequence [19] with data points of 2 K and 512 for the t_2 and t_1 dimensions, respectively. A one-dimensional (1D) NOE experiment was carried out with 0.5 s presaturation of the desired signal with 60 dB below a power of 0.5 W. 1D spectra of [^{15}N]^{1}H heteronuclear multiple quantum correlation (HMQC) with ^{15}N,^{13}C-decoupling [20] were obtained with an interpulse delay time of 4 ms. Protons were decoupled from ^{15}N during acquisition by a GARP sequence [21].

3. Results

3.1. Characterization of A. suum mt $tRNA^{Ser}_{UCU}$ and its transcript

In order to examine if the transcript of tRNA$^{Ser}_{UCU}$ is functionally equivalent to the native tRNA$^{Ser}_{UCU}$, their aminoacylation activity and binding activity to EF-Tu were examined. *A. suum* mt tRNA$^{Ser}_{UCU}$ and its transcript were serylated using *A. suum* mt extract (Fig. 3a), although its SerRS activity was very low. The serine accepting activity of the mt tRNA$^{Ser}_{UCU}$ transcript was slightly lower than the native one, however, they were almost identical (Fig. 3a). The low aminoacylation activity of both native tRNA$^{Ser}_{UCU}$ and the transcript may come from the structural instability of tRNA itself and/or the low activity of the *A. suum* mt extract. The EF-Tu binding activity of the tRNA$^{Ser}_{UCU}$ transcript was also observed using *T. thermophilus* EF-Tu (Fig. 3c), and was almost the same as the activity of the native one (Fig. 3b). Those biological data suggested that the transcript was fully employable as a substitute for the native tRNA$^{Ser}_{UCU}$.

The melting temperature (T_m) and hyperchromicity are

Table 2
Yields of ligation reactions

Labeled site	Yield of ligation reaction[a] (%)		Yield (mg)
	1st ligation	2nd ligation	
G8	62	42	0.92
U11	78	76	0.38
U30	46	17	0.29
U33	17	14	0.17
G34	41	49	0.28
G35	48	77	1.36
G37	74	56	0.25

[a]The yield after purification. '1st ligation' means the ligation of the 5′-fragment and the labeled nucleotide, and '2nd ligation' means the ligation of the product of the 1st ligation and the 3′-fragment.

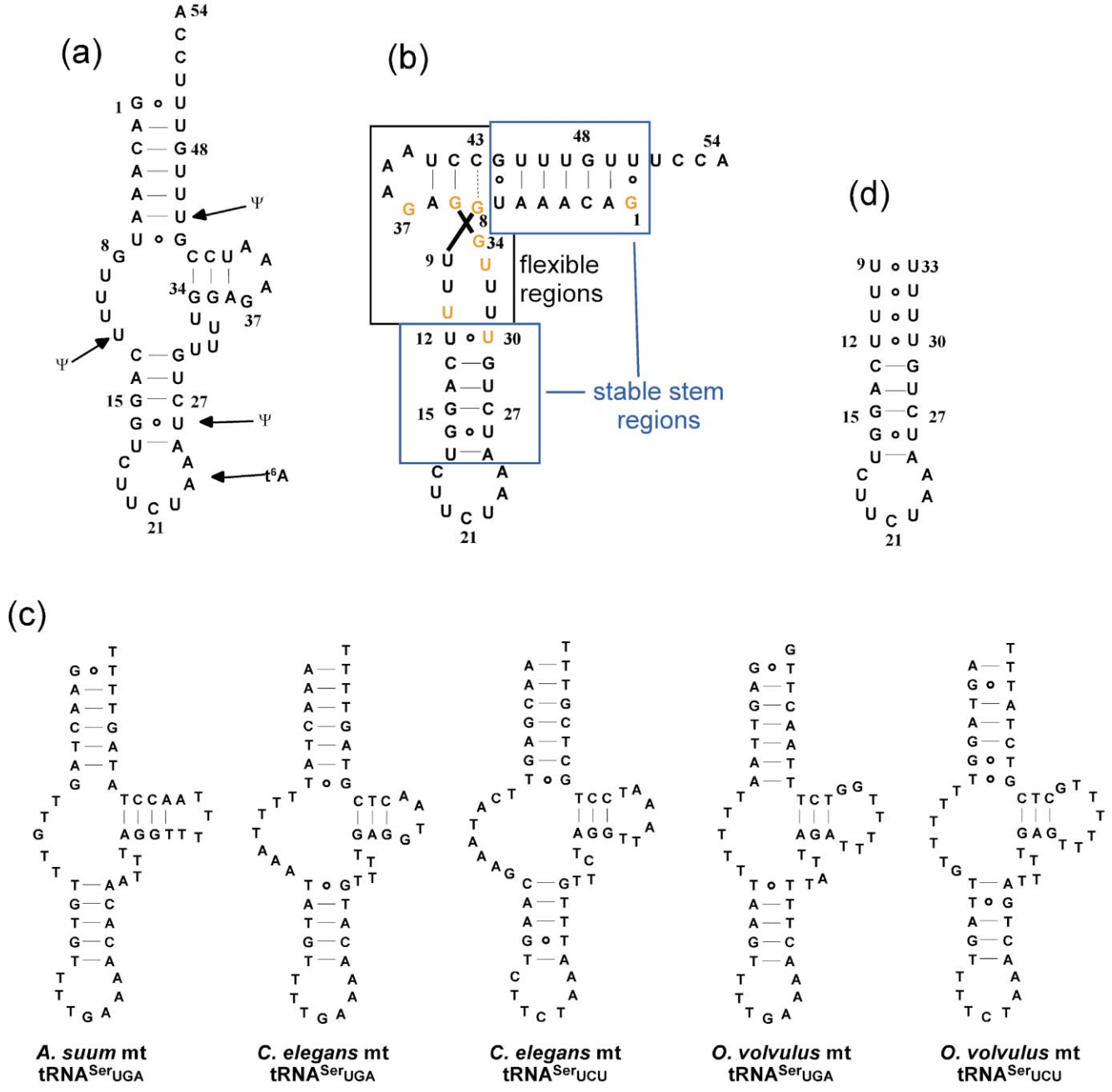

Fig. 1. a: Secondary structure of *A. suum* mt $tRNA^{Ser}_{UCU}$ [1]. Modified bases such as Ψ and t^6A are shown by arrows [4]. The numbering system of Sprintzl et al. [9] was not used here because $tRNA^{Ser}_{UCU}$ is extremely truncated tRNA. b: Secondary structural model of *A. suum* mt $tRNA^{Ser}_{UCU}$ proposed by this work. Isotopically labeled residues are shown in orange. c: Other nematode mt $tRNA^{Ser}$ genes [2,3,6]. d: A model of the 9 bp anticodon arm suggested by Steinberg et al. [12] is adapted to *A. suum* mt $tRNA^{Ser}_{UCU}$.

summarized in Table 3. The T_m value and hyperchromicity of *A. suum* mt $tRNA^{Ser}_{UCU}$ were remarkably lower than the standard yeast $tRNA^{Phe}$. The T_m value of the mt $tRNA^{Ser}_{UCU}$ transcript was slightly lower than the native one. Most likely, modified nucleosides (pseudouridine (Ψ) and N^6-threoninocarbonyl-adenosine (t^6A)) in the native tRNA (Fig. 1a) increased thermostability in comparison with the tRNA transcript. The stabilization of RNA stacking by Ψ was reported previously [22–25]. Slight stabilization by t^6A at the same position as *A. suum* mt $tRNA^{Ser}_{UCU}$ was observed using bovine mt $tRNA^{Ser}_{GCU}$ [26]. The T_m value of native bovine mt $tRNA^{Ser}_{GCU}$ having t^6A only as a modified nucleoside was 1.5°C higher than that of the $tRNA^{Ser}_{GCU}$ transcript [26]. However, considering the above biological activity, the modified bases were thought to have minor effects on the whole tertiary structure of *A. suum* mt $tRNA^{Ser}_{UCU}$.

3.2. NMR spectroscopy

Iminoproton signals were assigned by NOE data as shown in Fig. 4 and Table 4. All iminoproton signals in the acceptor stem and the anticodon stem except for the G1–U50 basepair were assigned from the NOE data. Iminoproton signals of the U12–U30 basepair were also assigned according to the NOE connectivity from G29 (Fig. 4a).

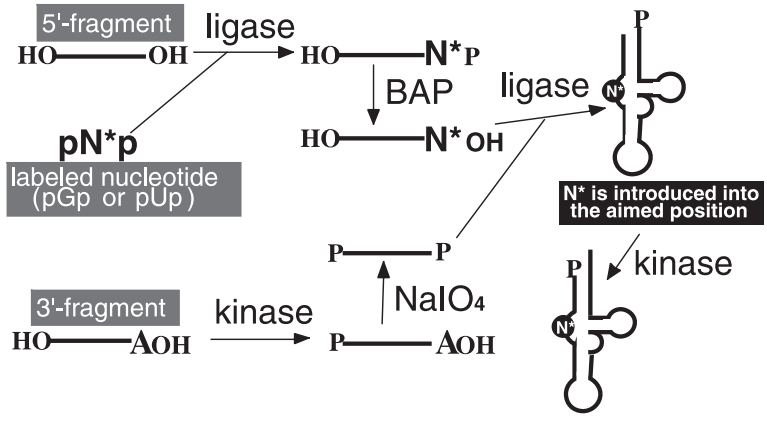

Fig. 2. Diagram showing how to construct site-specific labeled *A. suum* mt $tRNAs^{Ser}_{UCU}$. Asterisks denote ^{15}N,^{13}C-labeled nucleotides.

To clarify unassigned signals, site-specific stable isotope-labeled tRNAs were prepared by in vitro transcription with T7 RNA polymerase for G1 or enzymatic ligation for G8, U11, U30, U33, G34, G35 and G37. The ^{15}N-decoupled 1D spectra of all the labeled tRNAs coincided well with the spectrum of the non-labeled tRNA (Fig. 5), indicating that ligation at different positions caused no appreciable difference in the tertiary folding of the tRNAs. Although the iminoproton signal of G1 was not assigned from the NOE data, the signal was assigned in the 1D $[^{15}N]^1H$ HMQC spectrum (Fig. 5) of G1-labeled tRNA, and an NOE signal between G1 and U50 was detected in the NOESY spectrum (Fig. 4a). The U30 signal was confirmed by specific labeling (Fig. 5). An iminoproton signal of G35 was assigned using G35-labeled tRNA (Fig. 5). An NOE signal from the G35 signal was detected at 14.16 ppm by 1D NOE experiments (Fig. 4b) although it was not detected in the NOESY spectrum (Fig. 4a). Thus, this signal (14.16 ppm) should be the iminoproton signal of U41. As for G8, an iminoproton signal shift to a lower magnetic field was observed (Fig. 5), indicating that G8 was included in basepairing. Iminoproton signals of G34, U33 and U11 were not detected (Fig. 5), indicating that those were free from basepairing. The iminoproton signal of G37 (10.67 ppm) was observed at similar chemical shifts in the previously described NMR spectrum of the GAAA loop known as one of the extremely stable GNRA tetraloops [27,28]. A minor conformation of G37 existed because a minor signal was observed at 12.57 ppm. An NOE signal from G37 was not detected. Although the minor conformation of G37 (12.58 ppm), which seemed to pair with the other residue, was increased in the Mg^{2+} free condition (12.52 ppm), the majority was the signal at 10.50 ppm.

4. Discussion

In this study, an attempt using ^1H-NMR spectroscopy was made to elucidate the higher order structure of *A. suum* mt $tRNA^{Ser}_{UCU}$, which has been known until now as the shortest tRNA comprising 54 residues. At first, it was confirmed that the T7 transcript of the tRNA can be substituted for the native tRNA with regard to biological functions such as aminoacylation and binding ability to EF-Tu. Thus, the transcript was used as the sample for the NMR measurement, because preparation of the native tRNA from *A. suum* in amounts sufficient for the NMR measurement is quite difficult.

It was confirmed that the way of basepairing in both the acceptor and anticodon stems is just the same as that inferred from the cloverleaf structure (Fig. 1a) by the sequential assignment of iminoproton signals. It was also observed from the NOE pattern (Fig. 4a) that bases U12 and U30 were involved in basepairing and stacked on the C13–G29 pair of the anticodon stem. U11 and U31 also seemed to stack on the U12–U30 basepair because the iminoproton signals of U12 and U30 were observed unambiguously (Figs. 4a and 5), suggesting that the iminoprotons of U12 and U30 are protected from exchange with water protons.

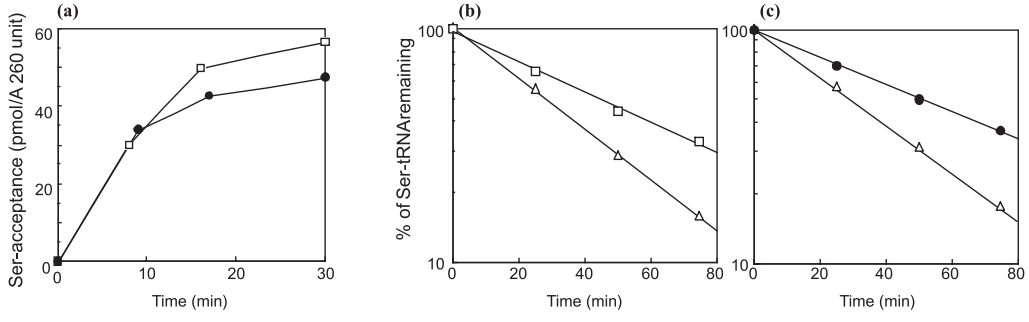

Fig. 3. Biological activity of the *A. suum* mt $tRNA^{Ser}_{UCU}$ transcript. a: Serine acceptance of native *A. suum* mt $tRNA^{Ser}_{UCU}$ (open square) and the $tRNA^{Ser}_{UCU}$ transcript (closed circle) by *A. suum* mt extract. b: Deacylation-protection assay of the aminoacyl ester bond against hydrolysis [16] of the native Ser-$tRNA^{Ser}_{UCU}$ (initially 30 nM) by *T. thermophilus* EF-Tu (open square) and no protein (open triangle). c: Deacylation-protection assay of the Ser-$tRNA^{Ser}_{UCU}$ transcript (initially 30 nM) by *T. thermophilus* EF-Tu (closed circle) and no protein (open triangle).

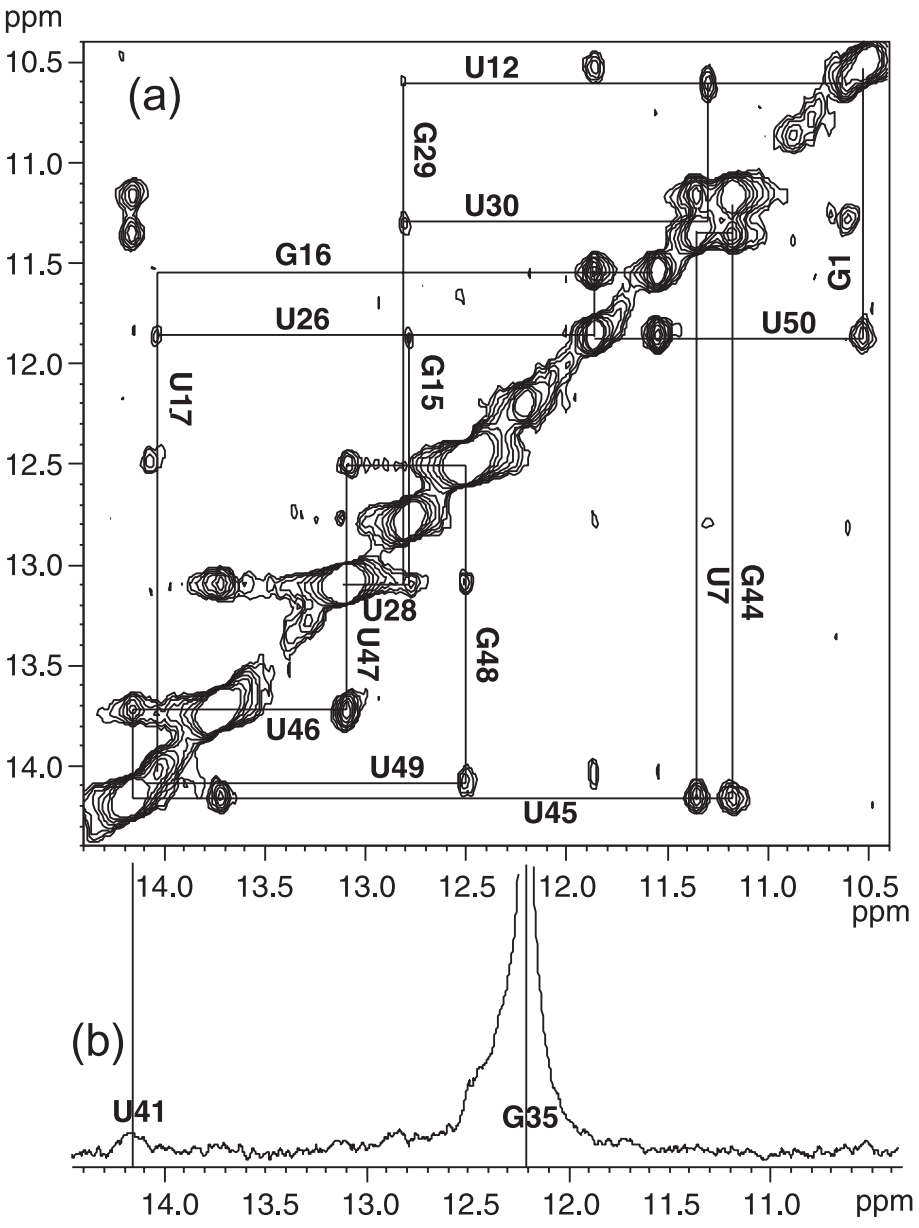

Fig. 4. NOE experiments using the unlabeled $tRNA^{Ser}_{UCU}$ at 283 K in the magnesium free condition. a: The NOESY spectrum. b: The NOE difference spectrum. Iminoproton signal of G35 was irradiated.

The assignment of iminoproton signals in the T stem was difficult because they were very weak. The weakness of the signals and the minor signals observed for G35 and G37 (Table 4) indicate that the T stem–loop is unstable. The T loop seemed to form the GAAA tetraloop [27,28], in which the iminoproton of the G37 residue is predominantly uninvolved in hydrogen bonding, because the chemical shift of the iminoproton signal of G37 (10.67 ppm) coincided with that of a free GAAA loop [27]. G34 and G35 existing in the T stem in the proposed secondary structure were site-specifically labeled with a stable isotope. An iminoproton signal of G35 was detected (Fig. 5) and a weak NOE signal from G35 to U41 was observed by the 1D NOE experiment (Fig. 4b). No signal was detected in the $[^{15}N]^1H$ HMQC spectrum of G34-labeled tRNA (Fig. 5), indicating that the G34–C43 basepair was neither rigid nor existent. On the other hand, an iminoproton signal of G8 was observed (Fig. 5) and its chemical shift was located in the typical G–C pair region. Thus, it is very likely that the G8–C43 basepair exists instead of the G34–C43, which is mostly expected according to the usual cloverleaf structure (Fig. 1a). This speculation leads to a rather unexpected secondary structure having the 1 bp shorter T stem and 1 bp longer acceptor stem (Fig. 1b). Such an unusual 8 bp acceptor stem has already been reported for *E. coli* $tRNA^{Sec}$

Table 3
Melting temperature and hyperchromicity of *A. suum* mt tRNAs and *E. coli* $tRNA^{Phe}$

tRNA	T_m (°C)	Hyperchromicity (%)
A. suum mt $tRNA^{Ser}_{UCU}$ (native)	54.5	21
A. suum mt $tRNA^{Ser}_{UCU}$ (transcript)	50	21
A. suum mt $tRNA^{Met}$ (native)	54.5	20
E. coli $tRNA^{Phe}$ (native)	76	31

Table 4
Assignment of iminoproton signals at 10°C

Position	Chemical shift (ppm)		NOE	Label
	0 mM $MgCl_2$	15 mM $MgCl_2$		
G1	10.53	10.45	U50	yes
U50	11.87	11.90	G1	
U49	14.08	–	G48	
G48	12.50	12.56	U49, U47	
U47	13.10	13.16	G48, U46	
U46	13.73	13.72	U47, U45	
U45	14.17	14.07	U46, G44, U7	
G44	11.17	11.20	U45, U7	
U7	11.35	11.32	U45, G44	
G8	12.73	12.96		yes
U33	–	–		yes
U11	–	–		yes
U12	10.60	10.60	U30, G29	
U30	11.29	11.31	U12, G29	yes
G29	12.81	12.86	U12, U30, U28	
U28	13.12	13.16	G29, G15	
G15	12.78	12.86	U28, G16, U26	
G16	11.54	11.51	G15, U26, U17	
U26	11.86	11.83	G15, G16, U17	
U17	14.05	13.93	U26	
G34	–	–		yes
G35	12.21 (10.32)	12.19	U41	yes
G37	10.50 (12.52)	10.67 (12.58)		yes
U41	14.16	–	G35	

Parentheses show minor signals.

[29], for example. As for the other nematode mt tRNAs^{Ser}, secondary structures reported previously [1–3], as shown in Fig. 1c, seem to be more appropriate than those with the 8 bp acceptor stem as shown in Fig. 1b, because in the latter cases it is almost impossible to replace U8–U or U8–C by a more stable U–A or C–G pair in the usual T stem. More information is necessary to clarify the existence of the G8–C43 pair.

The NOE connectivity of (U7–G44)–G8–G35 or (U7–G44)–G34–G35 as the basis for the direct connection of the acceptor stem to the T stem was not observed, which probably means that these two stems do not stack on each other. However, it is possible to consider that once the tRNA binds to EF-Tu, a coaxial helix composed of more than 10 bp could be formed between the acceptor and the T stems, because the nematode mt tRNA^{Ser} was shown to bind to *T. thermophilus* EF-Tu (Fig. 3b,c) whose minimal substrate is known to be the 10 bp minihelix [30]. These results concerning the acceptor–T stem connectivity are the same as those reported for bovine mt $tRNA^{Ser}_{GCU}$; although the NOE connectivity between the acceptor and the T stems was not observed [31], the $tRNA^{Ser}_{GCU}$ could bind *T. thermophilus* EF-Tu [32].

The regions covering U9 to U11 and U31 to U33 (here, a region formed by these residues is named a 'connector region') were indicated as being flexible and not basepaired because iminoproton signals of U11 and U33 were not observed (Fig. 5). These observations are consistent with the previous results of the enzymatic probing that RNase T_2 cleaved phosphodiester bonds of the 5′-side of U9, U10, U31, U32 and U33 but V_1 did not [4]. The extremely low thermostability of *A. suum* mt $tRNA^{Ser}_{UCU}$ (Table 3) is typical for mt tRNAs [26], in which *A. suum* mt tRNAs provides the most unstable examples. The low T_m value of *A. suum* mt $tRNA^{Ser}_{UCU}$ indicates the structural instability of the tRNA, which probably stems from the flexibility of the connector region and the T stem.

A structural model of the tRNA was manipulated using the MidasPlus software system [33], in which the acceptor stem and anticodon stem were fixed at the same positions as those

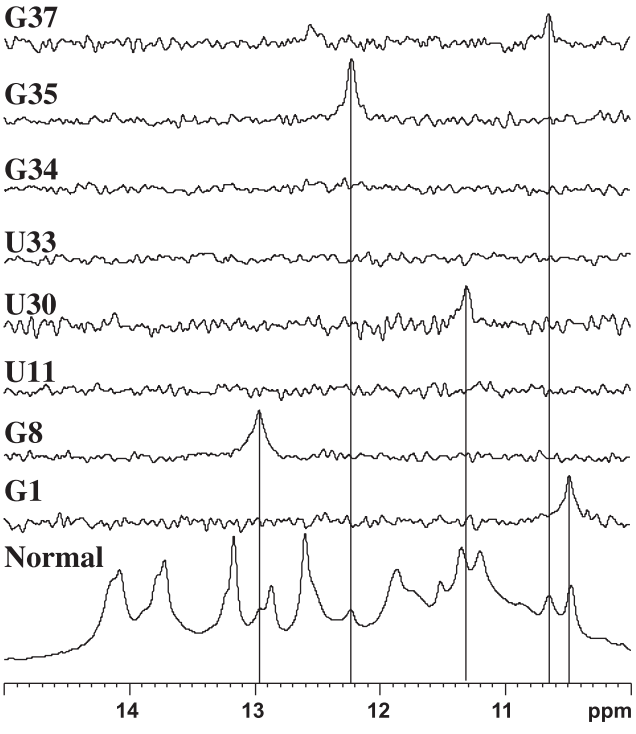

Fig. 5. 1D spectra of synthetic *A. suum* mt $tRNA^{Ser}_{UCU}$ recorded in the 15 mM $MgCl_2$ condition at 283 K. [^{15}N]^{1}H HMQC spectra of the tRNAs labeled at G37, G35, G34, U33, U30, U11, G8 and G1, and the normal spectrum of the unlabeled tRNA are shown.

of the standard L-shape structure of yeast $tRNA^{Phe}$ [34]. It turned out that the connector region was too short to connect the two stems naturally; the region was pulled away from the two stems, and bases continuing in the region could not stack on each other. To preserve the distance between the 3′-terminus and the anticodon in the ribosome, the acceptor–anticodon interstem angle of this tRNA should be larger than that of the standard L-shape tRNA, as described by Steinberg et al. [12]. However, the 9 bp anticodon stem (like Fig. 1d) suggested by Steinberg et al. [12] was not suggested in this tRNA, because basepairs including U9∼U11 and U31∼U33 were observed neither by NMR nor by enzymatic probing [4]. It is difficult to consider that the acceptor–anticodon interstem angle of the $tRNA^{Ser}_{UCU}$ is fixed by itself in an aqueous solution. The interstem angle should be fixed only when the tRNA is complexed with other factors, such as EF-Tu or the ribosome.

In this work, the structural features of *A. suum* mt $tRNA^{Ser}_{UCU}$ are shown, in which the stable stem regions and the flexible T stem and connector region were clarified (Fig. 1b). This tRNA seems to fit the ribosome by adjusting the distance between the 3′-terminus and the anticodon using the flexible connector region as suggested from the NMR data.

Acknowledgements: We would like to thank Dr. Y. Watanabe for discussions and the material, Dr. K. Kita (University of Tokyo, Japan) for the *A. suum* mitochondria and Dr. C. Takemoto for *E. coli* $tRNA^{Phe}$. This work was supported by Grants-in-Aid for Scientific Research on Priority Areas (No. 04272102 and No. 04272103) from the Ministry of Education, Science, Sports and Culture of Japan, JSPS (to T.O.) and by the Human Frontier Science Program Organization.

References

[1] Wolstenholme, D.R., Macfarlane, J.L., Okimoto, R., Clary, D.O. and Wahleithner, J.A. (1987) Proc. Natl. Acad. Sci. USA 84, 1324–1328.
[2] Okimoto, R. and Wolstenholme, D.R. (1990) EMBO J. 9, 3405–3411.
[3] Wolstenholme, D.R., Okimoto, R. and Macfarlane, J.L. (1994) Nucleic Acids Res. 22, 4300–4306.
[4] Watanabe, Y., Tsurui, H., Ueda, T., Furushima, R., Takamiya, S., Kita, K., Nishikawa, K. and Watanabe, K. (1994) J. Biol. Chem. 269, 22902–22906.
[5] Ohtsuki, T., Kawai, G. and Watanabe, K. (1998) J. Biochem. (Tokyo) 124, 28–34.
[6] Keddie, E.M., Higazi, T. and Unnasch, T.R. (1998) Mol. Biochem. Parasitol. 95, 111–127.
[7] Arcari, P. and Brownlee, G.G. (1980) Nucleic Acids Res. 8, 5207–5212.
[8] de Bruijn, M.H.L., Schreier, P.H., Eperon, I.C., Barrell, B.G., Chen, E.Y., Armstrong, P.H., Wong, J.F.H. and Roe, B.A. (1980) Nucleic Acids Res. 8, 5213–5222.
[9] Sprinzl, M., Horn, C., Brown, M., Ioudovitch, A. and Steinberg, S. (1998) Nucleic Acids Res. 26, 148–153.
[10] Noguchi, Y., Endo, K., Tajima, F. and Ueshima, R. (2000) Genetics 155, 245–259.
[11] Masta, S.E. (2000) Mol. Biol. Evol. 17, 1091–1100.
[12] Steinberg, S., Gautheret, D. and Cedergren, R. (1994) J. Mol. Biol. 236, 982–989.
[13] Ohtsuki, T., Kawai, G., Watanabe, Y., Kita, K., Nishikawa, K. and Watanabe, K. (1996) Nucleic Acids Res. 24, 662–667.
[14] Donis-Keller, H. (1980) Nucleic Acids Res. 8, 3133–3142.
[15] Ohtsuki, T., Vinayak, R., Watanabe, Y., Kita, K., Kawai, G. and Watanabe, K. (1996) J. Biochem. (Tokyo) 120, 1070–1073.
[16] Pingoud, A., Urbanke, C., Krauss, G., Peters, F. and Maass, G. (1977) Eur. J. Biochem. 78, 403–409.
[17] Ohtsuki, T., Watanabe, Y., Takemoto, C., Kawai, G., Ueda, T., Kita, K., Kojima, S., Kaziro, Y., Nyborg, J. and Watanabe, K. (2001) J. Biol. Chem. 276, 21571–21577.
[18] Plateau, P. and Guéron, M. (1982) J. Am. Chem. Soc. 104, 7310–7311.
[19] Macura, S. and Ernst, R.R. (1980) Mol. Phys. 41, 95–117.
[20] Bax, A., Griffey, R.H. and Hawkins, B.L. (1983) J. Magn. Reson. 55, 301–315.
[21] Shaka, A.J., Barker, P.B. and Freeman, R. (1985) J. Magn. Reson. 64, 547–552.
[22] Hall, K.B. and McLaughlin, L.W. (1991) Biochemistry 30, 1795–1801.
[23] Davis, D.R. and Poulter, C.D. (1991) Biochemistry 30, 4223–4231.
[24] Arnez, J.G. and Steitz, T.A. (1994) Biochemistry 33, 7560–7567.
[25] Davis, D.R. (1995) Nucleic Acids Res. 23, 5020–5026.
[26] Hayashi, I., Kawai, G. and Watanabe, K. (1998) J. Mol. Biol. 284, 57–69.
[27] Heus, H.A. and Pardi, A. (1991) J. Mol. Biol. 217, 113–124.
[28] Heus, H.A. and Pardi, A. (1991) Science 253, 191–194.
[29] Schön, A., Böck, A., Ott, G., Sprinzl, M. and Söll, D. (1989) Nucleic Acids Res. 17, 7159–7165.
[30] Rudinger, J., Blechschmidt, B., Ribeiro, S. and Sprinzl, M. (1994) Biochemistry 33, 5682–5688.
[31] Hayashi, I., Yokogawa, T., Kawai, G., Ueda, T., Nishikawa, K. and Watanabe, K. (1997) J. Biochem. (Tokyo) 121, 1115–1122.
[32] Gebhardt-Singh, E. and Sprinzl, M. (1986) Nucleic Acids Res. 14, 7175–7188.
[33] Ferrin, T.E., Huang, C.C., Jarvis, L.E. and Langridge, R. (1988) J. Mol. Graph. 6, 13–27.
[34] Rich, A. and Kim, S.-H. (1978) Sci. Am. 238, 56–62.